Environment International 178 (2023) 108032

Contents lists available at ScienceDirect

Environment International

journal homepage: www.elsevier.com/locate/envint

Full length article

# Impact of ultrafine particles and total particle number concentration on five cause-specific hospital admission endpoints in three German cities

Maximilian Schwarz [a,b,*], Alexandra Schneider [a], Josef Cyrys [a], Susanne Bastian [c], Susanne Breitner [a,b,1], Annette Peters [a,b,d,1]

[a] Institute of Epidemiology, Helmholtz Zentrum München - German Research Center for Environmental Health (GmbH), Neuherberg, Germany
[b] Institute for Medical Information Processing, Biometry and Epidemiology, Medical Faculty, Ludwig-Maximilians-Universität München, Munich, Germany
[c] Saxon State Office for Environment, Agriculture and Geology (LfULG), Dresden, Germany
[d] Department of Environmental Health, Harvard T.H. Chan School of Public Health, Boston, MA, USA

ARTICLE INFO

Handling Editor: Dr. Hanna Boogaard

*Keywords:*
Ambient air pollution
Ultrafine particles
Particle number concentrations
Particulate matter
Hospital admission
Morbidity

ABSTRACT

*Introduction:* Numerous studies have shown associations between daily concentrations of fine particles (e.g., particulate matter with an aerodynamic diameter ≤2.5 μm; $PM_{2.5}$) and morbidity. However, evidence for ultrafine particles (UFP; particles with an aerodynamic diameter of 10–100 nm) remains conflicting. Therefore, we aimed to examine the short-term associations of UFP with five cause-specific hospital admission endpoints for Leipzig, Dresden, and Augsburg, Germany.

*Material and methods:* We obtained daily counts of (cause-specific) cardiorespiratory hospital admissions between 2010 and 2017. Daily average concentrations of UFP, total particle number (PNC; 10–800 nm), and black carbon (BC) were measured at six sites; $PM_{2.5}$ and nitrogen dioxide ($NO_2$) were obtained from monitoring networks. We assessed immediate (lag 0–1), delayed (lag 2–4, lag 5–7), and cumulative (lag 0–7) effects by applying station-specific confounder-adjusted Poisson regression models. We then used a novel multi-level meta-analytical method to obtain pooled risk estimates. Finally, we performed two-pollutant models to investigate interdependencies between pollutants and examined possible effect modification by age, sex, and season.

*Results:* UFP showed a delayed (lag 2–4) increase in respiratory hospital admissions of 0.69% [95% confidence interval (CI): −0.28%; 1.67%]. For other hospital admission endpoints, we found only suggestive results. Larger particle size fractions, such as accumulation mode particles (particles with an aerodynamic diameter of 100–800 nm), generally showed stronger effects (respiratory hospital admissions & lag 2–4: 1.55% [95% CI: 0.86%; 2.25%]). $PM_{2.5}$ showed the most consistent associations for (cardio-)respiratory hospital admissions, whereas $NO_2$ did not show any associations. Two-pollutant models showed independent effects of $PM_{2.5}$ and BC. Moreover, higher risks have been observed for children.

*Conclusions:* We observed clear associations with $PM_{2.5}$ but UFP or PNC did not show a clear association across different exposure windows and cause-specific hospital admissions. Further multi-center studies are needed using harmonized UFP measurements to draw definite conclusions on the health effects of UFP.

## 1. Introduction

Over the last decades, numerous epidemiological studies have investigated the effects of ambient air pollution on adverse health effects. Especially gaseous pollutants such as nitrogen dioxide ($NO_2$) or ozone ($O_3$), and particulate matter (PM) have been associated with mortality (Chen and Hoek 2020; Orellano et al., 2020) and morbidity (Atkinson et al., 2014; Brunekreef et al., 2021). Since the 1990s, the smallest size fraction of ambient particulate air pollution, the ultrafine particles (UFP), have been hypothesized to differ in risk from larger particle size fractions (HEI Review Panel on Ultrafine Particles, 2013; Stone et al., 2017). However, only a few epidemiological studies have investigated the effects of UFP on cause-specific hospital admissions.

UFP have been conventionally classified as particles with an aerodynamic diameter ≤100 nm (=0.1 μm) and originate in urban air mainly from motor traffic exhaust, several nucleation processes, and

* Corresponding author at: Institute of Epidemiology - Helmholtz Zentrum München GmbH, Ingolstädter Landstr. 1, 85764 Neuherberg, Germany.
*E-mail address:* maximilian.schwarz@helmholtz-munich.de (M. Schwarz).
[1] Authors share last authorship.

https://doi.org/10.1016/j.envint.2023.108032
Received 3 April 2023; Received in revised form 7 June 2023; Accepted 9 June 2023
Available online 15 June 2023
0160-4120/© 2023 The Authors. Published by Elsevier Ltd. This is an open access article under the CC BY-NC-ND license (http://creativecommons.org/licenses/by-nc-nd/4.0/).

combustion in general (Morawska et al., 2008; Vu et al., 2015). They can be emitted directly as primary particles by combustion processes in, e.g., engines or formed as secondary particles by photochemical processes and condensation of gaseous precursors such as cooling exhaust gases (Morawska et al., 2008; Vu et al., 2015). Due to their small particle size, UFP have different physical characteristics than fine PM (PM with an aerodynamic diameter of $\leq$2.5 μm; $PM_{2.5}$). For example, they highly contribute to the particle number concentration but only marginally to total particle mass and exhibit a greater spatial variation than fine PM (HEI Review Panel on Ultrafine Particles 2013; Stone et al., 2017). Furthermore, UFP can reach the smallest regions of the respiratory tract, the alveoli. They have a high deposition efficiency and a slower respiratory tract clearance than larger particles (HEI Review Panel on Ultrafine Particles, 2013; Stone et al., 2017). Toxicological studies reported a high surface reactivity and large surface area per unit mass, enabling UFP to absorb chemical substances more easily; thus, UFP might be more hazardous than PM (Kwon et al., 2020).

To date, regulatory air quality monitoring focuses on $PM_{2.5}$ or $PM_{10}$ (PM with an aerodynamic diameter of $\leq$10 μm) and some gaseous pollutants (e.g., $NO_2$ and $O_3$) and does not include separate monitoring of UFP. Scientific and legislative challenges result from the complexity of involved processes, the more elaborate and costly measurement techniques, and the lack of standardized measurements (Cassee et al., 2019). Furthermore, no legal monitoring obligation (due to the lack of limit values for UFP) could prompt continuous measurements of UFP at network monitoring stations (Cassee et al., 2019). As a result, UFP are measured only at a few measurement stations over a longer time.

Although the overall evidence is still conflicting and insufficient, there is evidence that suggests an effect of UFP or total particle number concentrations (PNC) on cause-specific mortality (HEI Review Panel on Ultrafine Particles, 2013; Ohlwein et al., 2019) and morbidity (HEI Review Panel on Ultrafine Particles, 2013; Samoli et al., 2020; Stone et al., 2017). Moreover, two recent systematic reviews on hospital admissions identified children as a susceptible subgroup. In particular, children with respiratory diseases might be more vulnerable to the effects of UFP exposure, and asthma exacerbation may play an important role (da Costa e Oliveira et al., 2019; Li et al., 2019). However, so far, only three larger multi-city epidemiological studies have investigated the effects of UFP on hospital admissions. Lanzinger and colleagues found the highest associations with respiratory hospital admissions for a 6-day average in UFP concentration (Lanzinger et al., 2016). Samoli and colleagues reported no association between UFP and respiratory hospital admissions, although suggestive effects were seen among younger people (0–14 years) (Samoli et al., 2020). Similar results were reported by Lin and colleagues for modeled UFP concentrations associated with cardiovascular hospital admissions in New York State, USA (Lin et al., 2022).

A recent study analyzed the adverse health effects of UFP in terms of cause-specific mortality in three German cities between 2010 and 2017 that reported a delayed increased risk of respiratory mortality following UFP exposure (Schwarz et al., 2023).

Here, we investigated the association of daily ambient UFP concentrations and PNC with cause-specific hospital admissions, using data from the same project including multiple monitoring stations per city. In addition, we assessed the effects of particle size sub-fractions within the range of 10–800 nm. Further, we performed two-pollutant models to examine whether UFP and PNC showed effects independent of other pollutants. We also assessed whether age, sex, and season modified the effects of UFP and PNC on hospital admissions.

## 2. Material and methods

### 2.1. Hospital admission data

We retrieved daily counts of hospital admissions for the study period January 1, 2010, to December 31, 2017, for the three German cities Dresden, Leipzig, and Augsburg from official statistics. Only the primary diagnosis at hospital discharge was considered. The following five hospital admission endpoints were included according to the International Statistical Classification of Diseases and Related Health Problems, 10th revision (ICD-10 codes): cardiovascular diseases (I00-I99), heart diseases (I00-I52), cerebrovascular diseases (I60-I69), respiratory diseases (J00-J99), and lower respiratory tract infections (LRTI; J12-J18 & J20-J22). The raw data set was accessed via a workstation for visiting scientists at the Research Data Centre (RDC) of the Federal Statistical Office and Statistical Offices of the Federal States ([Hospital Statistics (EVAS 23131)], survey years [2010–2017], DOI: 10.21242/23131.2010.00.02.1.1.0 to 10.21242/23131.2017.00.02.1.1.0, own claculations). We selected only individuals who lived in the cities of Dresden, Leipzig, or Augsburg and were admitted to a hospital in the respective state of Saxony or Bavaria. Linkage was based on the hospital's state and the patient's official residency codes. Due to German data protection regulations, information on the hospital location is only available at the state rather than at the city levels. We assumed that people living in one city are also likely to be hospitalized in the same city/region, especially since we included only ordinary (no outpatient cases) and acute (no planned cases) hospital admissions. As a result, the final case numbers of each city represent the people living in one city that were hospitalized in the same city/region. We excluded cases hospitalized before the study period or with coded hospital admissions for which the underlying cause was unknown. In addition, the final data set also comprised information on biological sex (female, male) and age (six age categories: 0–17 years, 18–44 years, 45–64 years, 65–74 years, 75–84 years, and 85+ years). Finally, we retrieved population data for the three cities from official statistical yearbooks.

### 2.2. Environmental data

We obtained data from six fixed monitoring stations located in Augsburg, Dresden, and Leipzig: four urban background stations (Augsburg-Hochschule [AFH]; Dresden-Winckelmannstr. [DDW]; Leipzig-West [LWE]; Leipzig-TROPOS [LTR]), and two traffic-related stations (Dresden-Nord [DDN]; Leipzig-Mitte [LMI]). Supplementary Table 1 provides more information on the included measurement stations. We assumed that the exposure concentrations at the background stations represented the respective city populations, whereas the traffic-related stations better captured the effects of peak concentrations. All six locations contributed to the German Ultrafine Aerosol Network (GUAN) (Birmili et al., 2016), which included air pollutants not routinely monitored, such as black carbon (BC) or particle number concentrations in different size ranges (Birmili et al., 2015; Birmili et al., 2016; Sun et al., 2019). Each individual set of station-specific air pollution data was then assigned to the respective hospital admission data for the corresponding city. Using distance metrics or other exposure assignment methods was not possible because the relevant data (e.g., patient address data) were unavailable due to data protection regulations. A map of all GUAN stations, their station type, and further information on the network and the selected stations are provided in the supplement (Supplementary Fig. 1). In brief, monitoring stations met the following three criteria: i) an exposure profile representative for the urban population, ii) a sufficient number of cases in the cities, and iii) high comparability and standardization of the monitoring devices.

Number concentrations of UFP and PNC (10–800 nm) were considered exposures of primary interest. On an exploratory basis, we also analyzed size-fractioned particle number concentrations in the following ranges: 10–20 nm, 20–30 nm, 30–50 nm, 50–70 nm, and 70–100 nm and defined nucleation mode (10–30 nm; NuMP), Aitken mode (30–100 nm; AiMP), and accumulation mode particles (100–800 nm; AcMP). Black carbon (BC), nitrogen dioxide ($NO_2$), and fine particles ($PM_{2.5}$) were treated as exposures of secondary interest.

The setup of the monitoring devices has been described in detail elsewhere (Birmili et al., 2015; Birmili et al., 2016; Schwarz et al., 2023;

Sun et al., 2019). An overview of device characteristics at the stations can be found in Supplementary Table 2. In brief, particle size distribution (PSD) data was measured by a mobility particle size spectrometer (MPSS, TROPOS-design [manufacturer]) in the size range of 3–800 nm, with different configurations at the monitoring stations. Additional information, such as quality assurance and calibration procedures, has been published elsewhere (Pfeifer et al., 2014; Schladitz et al., 2014; Wiedensohler et al., 2012; Wiedensohler et al., 2018). BC mass concentrations were measured using multiangle absorption photometers (MAAP, Model 5012, Thermo Scientific) for the Saxon stations and an aethalometer (Type 8100, Thermo Fisher Scientific Inc.) for Augsburg. Further information on BC measurements can be found elsewhere (Birmili et al., 2015; Birmili et al., 2016) and in Supplementary Table 2. High-volume samplers (HVS, model DHA-80, DIGITEL Elektronik AG) measured $PM_{2.5}$ mass concentrations at the Saxon stations, and tapered element oscillating microbalances (TEOM, model 1400a incl. FDMS 8500, Rupprecht & Patashnick Co., and TEOM model 1405, Thermo Fisher Scientific Inc.) were used at the Augsburg site. In Augsburg, both TEOMs were equipped with a Filter Dynamics Measurement System (FDMS model 8500b, Thermo Fisher Scientific Inc.) to correct for losses of some volatile fractions of PM. Additional information on $PM_{2.5}$ and $NO_2$ measurements is available online at the German Environmental Agency website (https://www.env-it.de/stationen/public/open.do).

When applicable, hourly and daily averages were calculated for all air pollutants and measured meteorological variables (e.g., temperature, relative humidity, and barometric pressure) at each station if 75% of the data was available. In the main analysis, the imputation of missing data was not performed. Based on the daily averages, we calculated lagged exposure concentrations for the same day of the event (lag 0) and up to seven days before the event (lag 7). In addition, multi-day averages were calculated representing immediate (lag 0–1), delayed (lag 2–4, lag 5–7), and cumulative effects (lag 0–7). At the LTR station, only PSD and BC were available; consequently, this station was excluded from the $NO_2$ and $PM_{2.5}$ analyses. In addition, data on meteorology were extracted from another urban background station, LWE, showing high correlations between the two stations. $NO_2$ was not measured at the Augsburg station (AFH). Therefore, we selected $NO_2$ data from another urban background station (A-LfU: Augsburg - Bavarian State Office for the Environment) with comparable station characteristics and high correlations.

### 2.3. Statistical analysis

We calculated descriptive statistics for air pollutants and meteorological variables and counts of hospital admissions. Spearman correlation coefficients were used to assess temporal variations, with values $\geq$0.7 considered high correlations.

We used a two-stage modeling approach of site-specific risk estimates in the first stage and pooled estimates in the second stage to examine the association between air pollutants and cause-specific hospital admissions.

In the first stage, we calculated confounder-adjusted Poisson regression models that allow for overdispersion. A priori, we set up a general confounder model and included a log offset for annual population numbers for each station. Based on the previous UFIREG project (UFIREG Project 2014) and current literature, we included the following confounders in each site-specific model: time trend, day of the week, public holidays, vacation periods, relative humidity, and air temperature. For air temperature, we adjusted for high and low temperatures separately, according to Stafoggia et al. (2013). Briefly, this method allows for modeling different lag structures of heat and cold (Stafoggia et al., 2013). We used cubic regression splines with four degrees of freedom (DF) per year for the time trend and three DF for meteorological variables to account for non-linear confounding and temporal/seasonal variations. We focused primarily on immediate (lag 0–1), delayed (lag 2–4, lag 5–7), and cumulative (lag 0–7) effects and investigated single-lag models secondarily. We decided to use this modeling approach over distributed lag models (DLM), as multiple missing exposure data and low hospital admission counts could influence the statistical power.

In the second stage, we pooled the site-specific estimates using a novel random-effects meta-analytical method for environmental research (Sera et al., 2019; Sera and Gasparrini, 2022). This method accounted for different nested hierarchical structures of the data (e.g., geographical variation between cities and stations within a city). We included a random term for city and station and used restricted maximum likelihood (REML) estimation. Furthermore, we included the same analysis with fixed-effects models as an additional analysis. We examined potential heterogeneity among the station-specific estimates by calculating the $I^2$ statistic and the corresponding p-value. We considered $I^2 > 50\%$ and p-value $<0.05$ as substantial heterogeneity.

We performed further exploratory analyses only for the combination of air pollutants, lag structures, and hospital admission endpoints, showing the most adverse effect estimates in the main models. First, we obtained separate results for urban background and traffic-related sites to explore if the underlying exposure profiles showed different patterns. Second, we conducted two-pollutant models if the Spearman correlation coefficient between the two pollutants was less than 0.7. We included the second pollutant also as a linear term in the model and followed the general modeling strategy. Third, we examined possible effect modifications by age, sex, and season. Therefore, age- (0–17 years, 18–64 years, 65+ years) and sex-stratified (female, male) data was analyzed according to the main model. We included an interaction term to analyze the differences between warm (April-September) and cold periods (October-March). Finally, based on the literature, we used a fixed increment in air pollution concentration. This alternative standardization method facilitates comparison with the results of other epidemiological studies. We used 10,000 particles/$cm^3$ for all particle number concentrations (e.g., UFP or AiMP), 10 $\mu g/m^3$ for $PM_{2.5}$ and $NO_2$, and 1 $\mu g/m^3$ for BC mass concentrations.

### 2.4. Sensitivity analyses

We performed several sensitivity analyses to test the robustness of our main models.

I. We used 3 or 6 DF per year for time trend instead of 4 DF per year.
II. We increased the DF for air temperature and relative humidity terms to 5 DF (instead of 3 DF).
III. We replaced air temperature and relative humidity by apparent temperature (O'Neill et al., 2003; Wolf et al., 2009).
IV. We included barometric pressure as an additional variable in the main model.
V. We considered potential changes in hospital admissions due to influenza epidemics by including an influenza variable as an additional linear term for each city in the main model. In Germany, data on influenza epidemics data are publicly available at the Robert Koch Institute's database "SurvStat@RKI 2.0" (https://survstat.rki.de/default.aspx).
VI. For respiratory diseases (J00-J99), we excluded the following three ICD-10 codes because it could be assumed that these diagnoses involved planned hospital admissions:
    a. J32: Chronic sinusitis
    b. J34: Other diseases of the nose and paranasal sinuses
    c. J35: Chronic diseases of the palatine tonsils and pharyngeal tonsil
VII. We excluded the lower size fraction of 10–20 nm and created an alternate definition for UFP (20–100 nm) and PNC (20–800 nm). This was driven by potential measurement uncertainty in the lower range of PSD published by Wiedensohler et al. (2012).
VIII. We calculated city-specific exposure averages according to an adapted APHEA approach published by Berglind et al. (Berglind et al., 2009). Briefly, this method also included the imputation of missing values following a standardized procedure.

IX. Finally, we checked the exposure–response functions to investigate any deviations from linearity. Therefore, we replaced the linear term for the pollutant with a cubic regression spline with three DF, visually assessed the different slopes and compared the model output with a likelihood-ratio test.

To better compare the relative health effects of different air pollutants, we presented the results as percent change per interquartile range (IQR) increase in the respective pollutant along with the corresponding 95% confidence interval (CI). We provide a detailed description in the supplement together with fixed increment standardized main results. Results with a p-value less than 0.05 were considered statistically significant. All analyses and data management were performed using RStudio version 1.3.1335/1.4.1106 with R version 3.6.1/4.0.3 (The R Foundation for Statistical Computing, Vienna, Austria) and the R packages *mgcv* and *ggplot2*. The R package *mixmeta* was used for the second-stage analysis.

## 3. Results

### 3.1. Description of hospital admission data and air pollutants

The description of cause-specific hospital admissions and population numbers per city is presented in Table 1. Average daily cases ranged from 40.5 cases per day for cardiovascular hospital admissions for Leipzig to 3.2 cases per day for cerebrovascular hospital admissions for Augsburg. Table 2 describes the 24-hour-mean concentrations of air pollutants and meteorological variables; an extended version can be found in the supplement (Supplementary Table 3). The highest median UFP concentrations were measured at the traffic-related stations LMI and DDN with 10,123 particles/cm$^3$ and 8,637 particles/cm$^3$, respectively. The concentrations at the urban background stations ranged from 4,520 particles/cm$^3$ for LWE to 5,655 particles/cm$^3$ at AFH (Table 2). A similar pattern, but with higher concentrations, was observed for PNC.

**Table 1**
Description of the population living in one city that was hospitalized in the same city/area. N = 2922 days.

| Variable | Leipzig | Dresden | Augsburg |
|---|---|---|---|
| Mean population 2010–2017 | 542,918 | 534,382 | 279,159 |
| Total counts of cardiovascular disease HA. | 118,265 | 97,508 | 59,230 |
| Total counts of heart disease HA. | 81,323 | 68,711 | 40,582 |
| Total counts of cerebrovascular disease HA. | 14,955 | 14,121 | 9,434 |
| Total counts of respiratory disease HA. | 51,383 | 45,271 | 38,396 |
| Total counts of LRTI HA. | 17,801 | 14,489 | 13,467 |
| Mean daily cardiovascular disease HA. (SD) | 40.5 (16.7) | 33.4 (12.4) | 20.3 (8.7) |
| Mean daily heart disease HA. (SD) | 27.8 (11.2) | 23.5 (8.9) | 13.9 (6.3) |
| Mean daily cerebrovascular disease HA. (SD) | 5.1 (2.6) | 4.8 (2.4) | 3.2 (2.0) |
| Mean daily respiratory disease HA. (SD) | 17.6 (7.8) | 15.5 (6.6) | 13.1 (7.0) |
| Mean daily LRTI HA. (SD) | 6.1 (3.4) | 5.0 (3.0) | 4.6 (2.9) |

N: Number of days with valid data; HA: Hospital admission; SD: Standard deviation; LRTI: Lower respiratory tract infections; Population data based on official statistical yearbook of the cities, own calculations; Cardiovascular disease: ICD-10: I00-I99; Heart disease: ICD-10: I00-I52; Cerebrovascular disease: ICD-10: I60-J69; Respiratory disease: ICD-10: J00-J99; LRTI disease: ICD-10: J12-J18 & J20-J22; Source: Research Data Centre of the Federal Statistical Office and Statistical Offices of the Federal States ([Hospital Statistics (EVAS 23131)], survey years [2010–2017], DOI: 10.21242/23131.2010.00.02.1.1.0 to 10.21242/23131.2017.00.02.1.1.0, own claculations).

Compared to the routinely monitored air pollutants $NO_2$ and $PM_{2.5}$, the particle number concentrations and BC exhibited a higher percentage of missing values.

UFP and PNC were highly correlated (correlation coefficients between 0.96 and 0.98) but showed mostly weak to moderate correlations with the other pollutants and meteorological variables (Supplementary Table 4). In addition, UFP and PNC were moderately correlated between stations, with a clear pattern observed indicating higher correlations between stations for larger particle size fractions and $PM_{2.5}$ (Supplementary Table 5). Compared to UFP, higher correlations between PNC and BC, $NO_2$, and $PM_{2.5}$ were observed.

### 3.2. Air pollution and cause-specific hospital admissions

Fig. 1 (and Supplementary Table 6) displays the results of the pooled main models. UFP or PNC did not show a clear pattern across different exposure windows and hospital admission endpoints. However, results suggested a slight increase in cardiovascular hospital admissions and hospital admissions for heart diseases on the same day or one day after UFP exposure (lag 0–1). An interquartile range increase of 3,420 particles/cm$^3$ in UFP concentration resulted in a 0.43% [95% CI: −0.25%; 1.12%] higher risk of cardiovascular hospital admissions ($I^2 = 30.60\%$, $p = 0.206$). The effects of UFP on respiratory hospital admissions showed a delayed pattern with a 0.69% [95% CI: −0.28%; 1.67%] increased risk per 3,220 particles/cm$^3$ 2 to 4 days after exposure ($I^2 = 25.10\%$, $p = 0.246$). Comparable results were observed for PNC. For cerebrovascular hospital admissions and LRTI hospital admissions, mostly null results were seen.

We observed clearer association patterns for size-fractioned exposures (Fig. 2 and Supplementary Table 7). Results indicated increases in cardiovascular hospital admissions, hospital admissions for heart diseases, and respiratory hospital admissions in association with delayed and cumulative exposures to particles in the Aitken mode size ranges (NC 50–70 nm and NC 70–100 nm). In addition, we observed immediate, delayed, and cumulative pattern effects of particles in the accumulation mode (e.g., lag 0–7: cardiovascular hospital admissions: 1.20% [95% CI: 0.66%; 1.73%]; hospital admissions for heart diseases: 1.13% [95% CI: 0.54%; 1.72%]). For respiratory hospital admissions, an increase in risk was observed for larger size fractions 2 to 4 days after exposure (e.g., AcMP 1.55% [95% CI: 0.86%; 2.25%]), but size fractions in the ultrafine range also indicated higher risks (e.g., NC 70–100 nm 1.37% [95% CI: −0.24%; 3.00%]). For cerebrovascular hospital admissions, results indicated immediate and cumulative patterns for accumulation mode particles, whereas for LRTI hospital admissions, mostly null results were seen.

When we used fixed-effects instead of random-effects models, the direction and effect sizes did not change substantially (see Supplementary Figs. 2 and 3 and Supplementary Tables 8 and 9). However, considerably more associations reached statistical significance indicating that our main analysis using random-effects models can be considered rather conservative in terms of model interpretation and that accounting for hierarchical structures in the data by random structures (differences within and between cities) may be useful when pooling the station-specific effects of UFPs. It is important to note that substantial heterogeneity was observed mainly for cerebrovascular hospital admissions, cardiovascular hospital admissions and particles in the nucleation mode, or respiratory hospital admissions and particle size fractions in the Aitken mode (Supplementary Tables 8 and 9).

Single-lag and station-specific results for respiratory and cardiovascular hospital admissions can be found in Supplementary Fig. 4 and Supplementary Table 10. The results generally showed higher risks at lag 2 or lag 3 for respiratory hospital admissions. For cardiovascular hospital admissions, patterns can be seen for smaller particle sizes at immediate lags (e.g., lag 0), but also for delayed lags (e.g., lag 2 or lag 6) and larger size fractions (Supplementary Fig. 4). In addition, the results were mainly influenced by the Leipzig stations (Supplementary

**Table 2**
Basic descriptive statistics of air pollution and environmental data per measurement station.

| Variable | $N_{days}$ | Min. | Max. | Mean | SD | Median | IQR |
|---|---|---|---|---|---|---|---|
| UFP (10–100 nm, n/cm$^3$) | | | | | | | |
| LMI | 2,279 | 2,212 | 35,987 | 10,747 | 4,172 | 10,123 | 5,156 |
| LWE | 1,787 | 931 | 21,681 | 5,126 | 2,619 | 4,520 | 3,003 |
| LTR | 2,668 | 798 | 32,917 | 5,469 | 2,881 | 4,839 | 3,154 |
| DDN | 2,287 | 2,100 | 24,781 | 9,128 | 3,436 | 8,637 | 4,366 |
| DDW | 2,211 | 705 | 22,526 | 5,341 | 2,754 | 4,791 | 3,156 |
| AFH | 2,392 | 953 | 49,075 | 6,366 | 3,621 | 5,655 | 3,514 |
| PNC (10–800 nm, n/cm$^3$) | | | | | | | |
| LMI | 2,279 | 2,632 | 38,180 | 12,590 | 4,692 | 11,922 | 5,866 |
| LWE | 1,787 | 1,288 | 23,362 | 6,265 | 2,886 | 5,748 | 3,482 |
| LTR | 2,668 | 1,054 | 34,927 | 6,703 | 3,231 | 6,054 | 3,686 |
| DDN | 2,287 | 2,450 | 30,684 | 10,912 | 3,924 | 10,292 | 4,975 |
| DDW | 2,211 | 941 | 24,714 | 6,714 | 3,184 | 6,186 | 3,902 |
| AFH | 2,392 | 1,214 | 51,597 | 7,668 | 4,113 | 6,909 | 4,017 |
| BC (μg/m$^3$) | | | | | | | |
| LMI | 2,499 | 0.4 | 10.9 | 2.3 | 1.2 | 2.0 | 1.3 |
| LWE | 2,067 | 0.1 | 10.1 | 1.0 | 0.9 | 0.8 | 0.8 |
| LTR | 2,807 | 0.0 | 12.6 | 1.0 | 1.0 | 0.7 | 0.8 |
| DDN | 2,693 | 0.3 | 11.5 | 1.8 | 1.0 | 1.5 | 1.1 |
| DDW | 2,057 | 0.1 | 7.4 | 0.9 | 0.7 | 0.7 | 0.8 |
| AFH | 2,644 | 0.5 | 10.5 | 1.7 | 1.0 | 1.4 | 1.0 |
| $NO_2$ (μg/m$^3$) | | | | | | | |
| LMI | 2,886 | 11.0 | 100.0 | 44.0 | 12.7 | 43.0 | 17.0 |
| LWE | 2,896 | 3.0 | 66.0 | 17.6 | 8.9 | 16.0 | 11.0 |
| LTR* | 0 | – | – | – | | – | |
| DDN | 2,874 | 9.0 | 77.0 | 34.2 | 10.4 | 33.0 | 14.0 |
| DDW | 2,890 | 3.0 | 72.0 | 20.2 | 9.5 | 18.0 | 12.0 |
| AFH | 2,212 | 2.5 | 84.0 | 19.8 | 10.2 | 17.7 | 12.3 |
| $PM_{2.5}$ (μg/m$^3$) | | | | | | | |
| LMI | 2,891 | 2.2 | 120.8 | 17.5 | 13.0 | 13.6 | 12.2 |
| LWE | 2,885 | 1.0 | 111.2 | 13.5 | 12.0 | 9.6 | 10.5 |
| LTR* | 0 | – | – | – | | – | |
| DDN | 2,900 | 1.9 | 137.8 | 16.2 | 12.6 | 12.3 | 11.6 |
| DDW | 2,892 | 0.5 | 136.4 | 15.1 | 12.9 | 10.9 | 12.3 |
| AFH | 2,922 | 1.1 | 98.7 | 13.0 | 10.3 | 10.2 | 10.3 |
| Air temperature (°C) | | | | | | | |
| LMI | 2,911 | −14.0 | 32.1 | 11.7 | 8.0 | 11.4 | 12.1 |
| LWE | 2,919 | −15.0 | 29.2 | 9.9 | 7.7 | 9.7 | 11.7 |
| LTR* | 0 | – | – | – | | – | |
| DDN | 2,915 | −14.2 | 31.8 | 11.4 | 8.1 | 11.3 | 12.5 |
| DDW | 2,922 | −13.4 | 31.0 | 11.6 | 8.0 | 11.6 | 12.4 |
| AFH | 2,803 | −13.4 | 28.9 | 9.9 | 7.9 | 9.9 | 12.3 |
| Relative humidity (%) | | | | | | | |
| LMI | 2,909 | 34.5 | 98.5 | 70.9 | 12.6 | 71.8 | 19.6 |
| LWE | 2,905 | 37.5 | 100.0 | 74.2 | 12.2 | 75.3 | 18.6 |
| LTR* | 0 | – | – | – | – | – | |
| DDN | 2,915 | 37.5 | 100.0 | 70.6 | 11.4 | 70.9 | 16.8 |
| DDW | 2,922 | 36.0 | 97.2 | 70.8 | 11.4 | 71.8 | 17.3 |
| AFH | 2,803 | 39.6 | 100.0 | 77.8 | 12.7 | 79.2 | 20.3 |
| Barometric pressure (hPa) | | | | | | | |
| LMI | 2911 | 975.0 | 1040.0 | 1015.8 | 8.1 | 1016.0 | 10.0 |
| LWE | 2919 | 975.0 | 1041.0 | 1016.1 | 8.3 | 1016.0 | 10.0 |
| LTR* | 0 | – | – | – | – | – | – |
| DDN | 2915 | 976.0 | 1042.0 | 1016.2 | 8.2 | 1016.0 | 10.0 |
| DDW | 2922 | 976.0 | 1041.0 | 1016.0 | 8.0 | 1016.0 | 10.0 |
| AFH | 2803 | 923.9 | 984.5 | 961.0 | 7.4 | 961.4 | 9.0 |

$N_{days}$: Number of days with valid data; Min.: Minimum; Max.: Maximum; SD: Standard deviation; IQR: Interquartile range; UFP: Particle number concentration of particles in the ultrafine range (10–100 nm); LMI: Leipzig-Mitte; LWE: Leipzig-West; LTR: Leipzig-TROPOS; DDN: Dresden-Nord; DDW: Dresden-Winckelmannstr.; AFH: Augsburg-Hochschule; PNC: Total particle number concentration (10–800 nm); BC: Black carbon; $NO_2$: Nitrogen dioxide; $PM_{2.5}$: Particulate matter with an aerodynamic diameter $\leq$ 2.5 μm; °C: Degree Celsius; hPa: hectopascal. *: No data available.

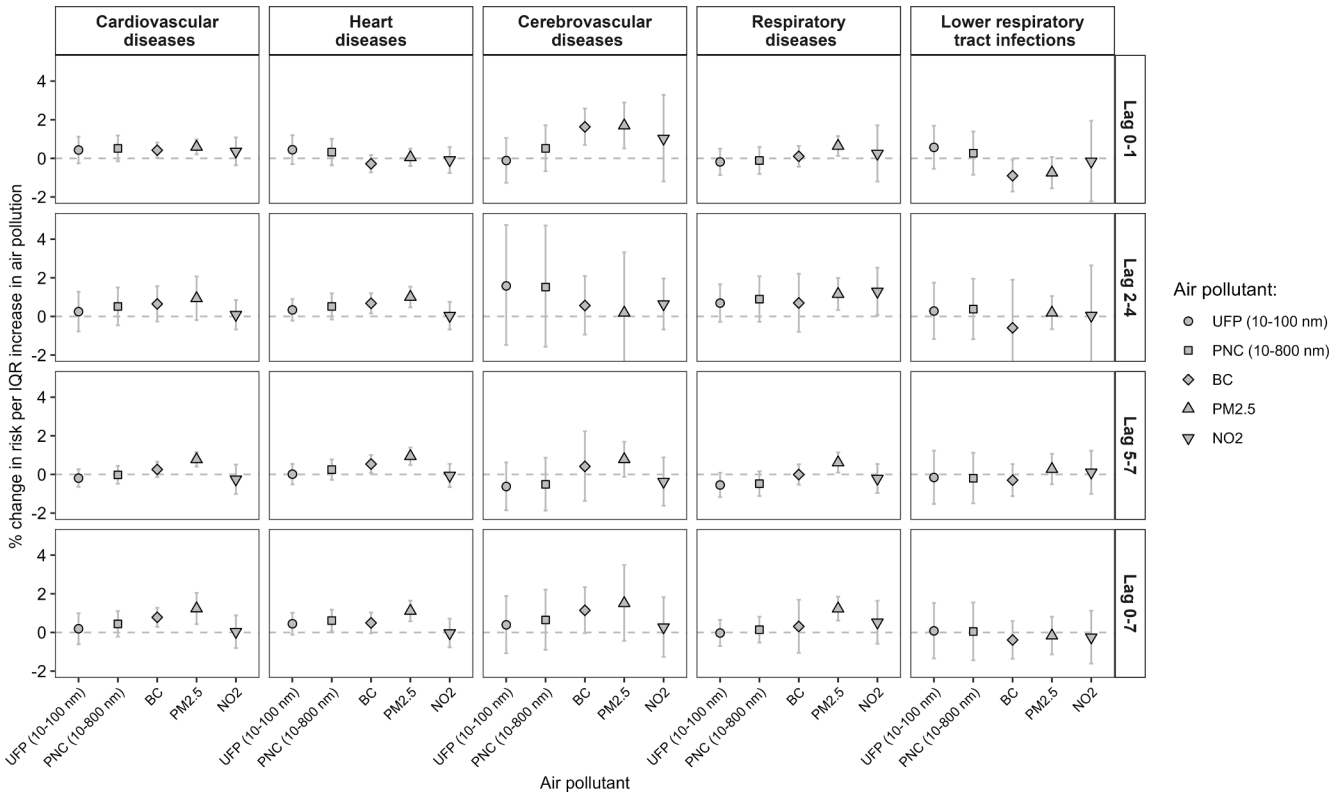


**Fig. 1.** Percent changes in the relative risk and 95% confidence interval per interquartile range (IQR: difference between the 75th and 25th percentile; corresponds to the spread of the middle 50% of the data) increases in air pollutants for cardiovascular disease- (left), heart disease- (second from left), cerebrovascular disease- (middle), respiratory disease- (second from right), and lower respiratory tract infection hospital admission (right). Standardization by IQR facilitates comparison between different pollutants. The x-axis and the shape show the type of pollutant. The y-axis represents the percent change of risk per interquartile range increase in air pollution concentration (left side) per average lag concentration of air pollutants (right side). All estimates represent the pooled analysis of the measurement stations using multi-level random-effects models, adjusted for main model covariates.

Table 10). Furthermore, an exploratory comparison of risks between urban background and traffic-related stations indicated comparable results, although the results indicated slightly higher associations at the traffic-related stations (Supplementary Figure 5 and Supplementary Table 11).

For both BC and $PM_{2.5}$, we found the most consistent associations with cause-specific hospital admissions for cardiovascular and cerebrovascular hospital admissions in association with immediate (lag 0–1) exposures, and for cardiovascular hospital admissions and hospital admissions for heart diseases for delayed (lag 5–7) and cumulative (lag 0–7) exposures. For example, an increase of 0.77 μg/m$^3$ in BC (lag 0–7) was associated with a 0.78% [95% CI: 0.29%; 1.27%] higher risk of cardiovascular hospital admissions (Fig. 1 and Supplementary Table 6). All four $PM_{2.5}$ average lags were associated with respiratory hospital admissions (e.g., lag 2–4: 1.16% [95% CI: 0.33%; 1.99%]), showing consistent results with the association patterns for the larger particle size fractions. $NO_2$ was not associated with any cause-specific hospital admissions, except for respiratory hospital admissions at lag 2–4, where an increase of 11.00 μg/m$^3$ was associated with a 1.29% [95% CI: 0.07%; 2.52%] higher risk (Fig. 1 and Supplementary Table 6).

### 3.3. Two-pollutant models and effect modification

We examined two-pollutant models and effect modification analyses for the combination of UFP exposure, average lag concentration, and hospital admission endpoint, for which the most consistent and strongest results were found in the main analysis. Fig. 3 and Supplementary Table 12 provide an overview of the results. The UFP effects on respiratory hospital admissions (lag 2–4) remained relatively stable and unchanged after additional adjustments for BC or $PM_{2.5}$. In particular, for $PM_{2.5}$, the smaller confidence intervals suggested independent, although insignificant, results. Further adjustment for $NO_2$ resulted in lower effect estimates and null effects. However, high correlations between UFP and $NO_2$ at station Leipzig-Mitte (LMI) restricted us from including this station in the pooled analysis.

There were no substantial differences in risks between women and men. For respiratory hospital admissions, higher risks were indicated for the younger age groups. Although not significant, children and adolescents had the largest point estimates for UFP exposure (age 0–17: 2.54% [95% CI: −0.47%; 5.63%] vs. age 65+: −0.19% [95% CI: −1.11%; 0.75]). An increase in the UFP concentration by 3,220 particles/cm$^3$ resulted in a 1.47% [95% CI: 0.25%; 2.70%] higher risk for respiratory hospital admissions in the cold season (Oct.-Mar.) (vs. Apr.-Sep.: −0.54% [95% CI: −1.55%; 0.48%]; Fig. 3 and Supplementary Table 12). In general, PNC showed comparable results for the two-pollutant and effect modification analyses. An alternative standardization with fixed-unit increments can be found in Supplementary Table 13 and 14, and Supplementary Figs. 6 and 8.

### 3.4. Sensitivity analysis

The results of the sensitivity analysis can be found in Fig. 4 and in the supplement and are presented again for the combination of UFP exposure, hospital admission endpoint, and average lag concentration with the most consistent and strongest results in the main analysis. Adjusting the model parameters did not substantially change the results, although setting the degrees of freedom for the long-term trend to three led to higher and significant results (Fig. 4). Similarly, we observed no changes when additionally adjusting for influenza, barometric pressure, or apparent temperature in the main model. The exclusion of three ICD-10

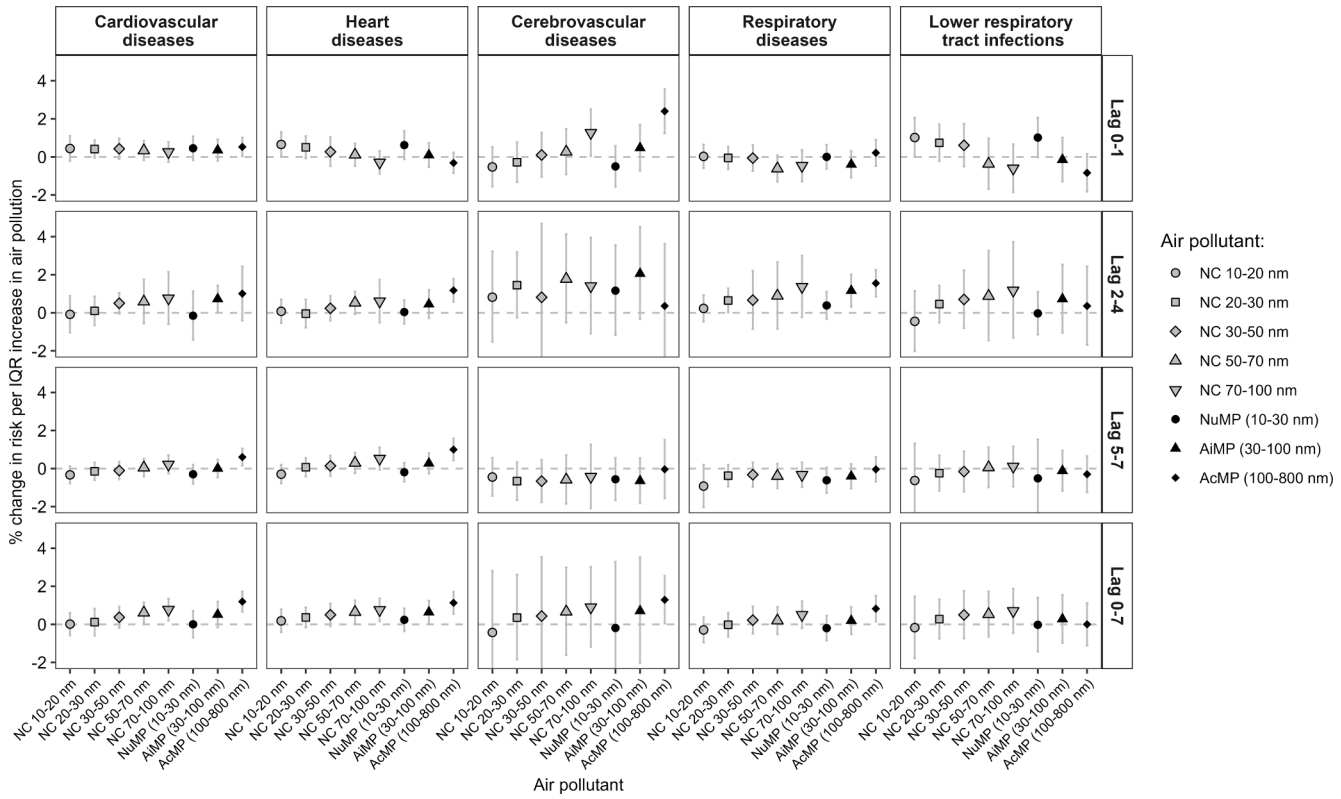


**Fig. 2.** Percent changes in the relative risk and 95% confidence interval per interquartile range (IQR: difference between the 75th and 25th percentile; corresponds to the spread of the middle 50% of the data) increases in air pollutants for cardiovascular disease- (left), heart disease- (second from left), cerebrovascular disease- (middle), respiratory disease- (second from right), and lower respiratory tract infection hospital admission (right). Standardization by IQR facilitates comparison between different pollutants. The x-axis and the shape show the type of pollutant. The y-axis represents the percent change of risk per interquartile range increase in air pollution concentration (left side) per average lag concentration of air pollutants (right side). All estimates represent the pooled analysis of the measurement stations using multi-level random-effects models, adjusted for main model covariates.

codes (potentially representing planned hospital admissions) yielded similar results. When an alternate definition for UFP or PNC was used (setting the lower cut-off values from 10 nm to 20 nm), the results changed only marginally from 0.69% [95% CI: −0.28%; 1.67%] (UFP 10–100 nm) to 0.90% [95% CI: −0.68%, 2.50%] (UFP 20–100 nm; Supplementary Table 15). Nevertheless, there was significant heterogeneity between the stations, particularly for lag 2–4 and respiratory hospital admissions (Supplementary Table 15). City-specific average concentrations generally resulted in smaller effect sizes and wider confidence intervals, although most results were comparable, especially for the larger particle size fractions and $PM_{2.5}$ (Supplementary Figure 9). Visual inspection of the exposure–response function showed no major deviations from linearity, although a likelihood-ratio test indicated significant differences between the linear and nonlinear models for the stations LWE and AFH (Supplementary Figure 10).

## 4. Discussion

This time-series analysis found no clear association between UFP or PNC and five cause-specific hospital admission endpoints. However, the results suggested delayed patterns for respiratory hospital admissions 2 to 4 days after exposure. Size-fractioned analyses showed more pronounced delayed and cumulative effects of Aitken mode and accumulation mode particles on cardiovascular hospital admissions, hospital admissions for heart disease, and respiratory hospital admissions, and the most consistent results for the larger particles $PM_{2.5}$. At the same time, more immediate patterns were found for smaller fractions. The results indicated higher risks for children and adolescents compared to the elderly, and higher risks in the cold season compared to the warm season, whereas the risk was comparable for men and women. Further adjustment for $PM_{2.5}$ and BC did not change the results for respiratory hospital admissions; adjustment for $NO_2$ led to null results.

To date, there is still limited evidence on UFP or PNC effects on hospital admissions, and only two multi-center studies have investigated this research question. A study conducted in five northern and southern European cities (Samoli et al., 2016a) reported no clear association between UFP exposure and respiratory hospital admissions. However, higher delayed risks were found for pooled single lags 3, 5, and 6, although significant heterogeneity was observed (e.g., lag 3 and respiratory HA: 0.43% [95% CI: −0.94%; 1.83%]) (Samoli et al., 2016a). In addition, point estimates increased when cities with no measured accumulation mode particles were excluded, although they remained insignificant (Samoli et al., 2016a). This observation is consistent with our findings of stronger effects for larger particle size fractions, especially for accumulation mode particles. Despite some methodological differences between our study and the study by Samoli and colleagues (e.g., different statistical methods, lag periods, or study area), we found comparable results that overall suggest patterns of delayed UFP effects on respiratory hospital admissions. In addition, both analyses suggest that the strongest effects are seen in children. Another multi-city study in five central and eastern European countries (Lanzinger et al., 2016) found a higher risk of respiratory hospital admissions, most strongly for a 6-day average UFP exposure. An increase of 2,750 particles/$cm^3$ was associated with a 3.40% [95% CI: −1.70%; 8.80%] increase in the risk of respiratory hospital admissions. Effects were generally higher for PNC, and no clear association was observed for cardiovascular hospital admissions (Lanzinger et al., 2016). Two stations of the study by Lanzinger et al. were also part of our study (AFH and DDW). We saw comparable results, although with smaller effect sizes but higher precision (narrower confidence intervals), probably due to the longer time series. However,

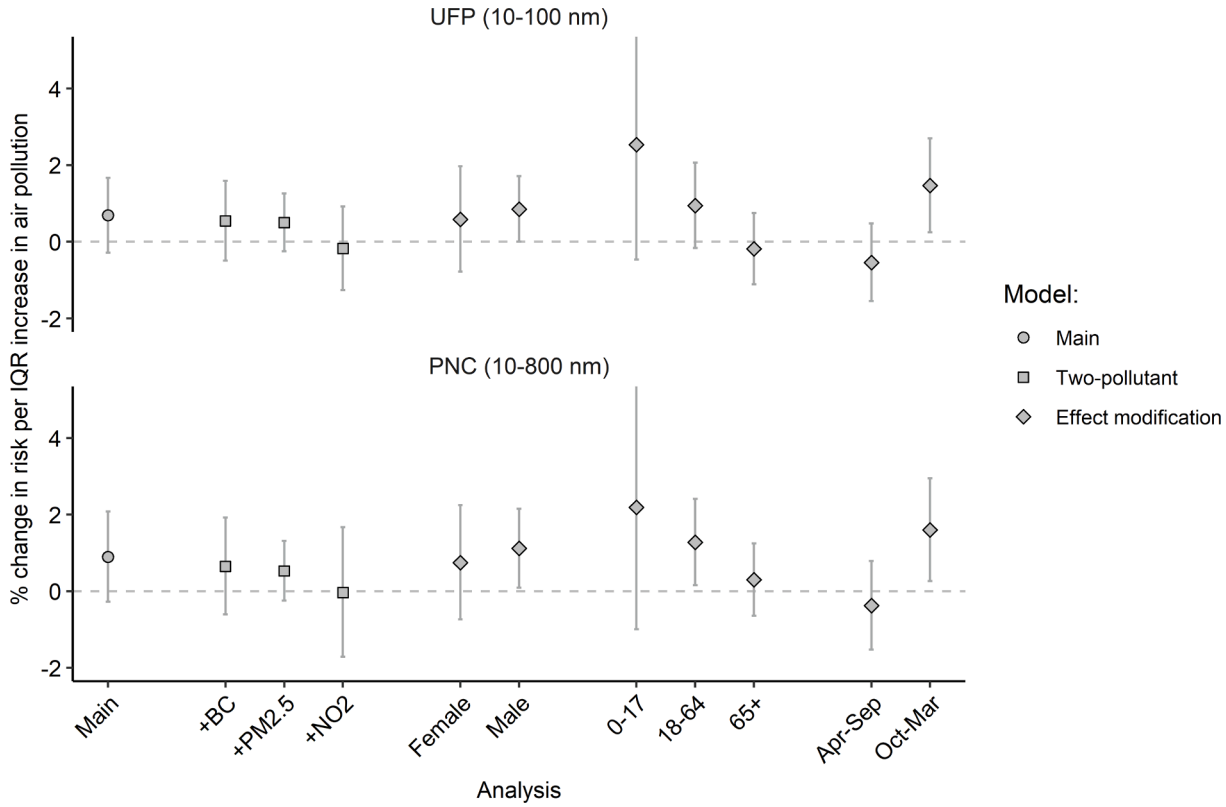


**Fig. 3.** Percent changes in the relative risk of respiratory hospital admission and 95% confidence intervals per interquartile range increases in ultrafine particles (10–100 nm; UFP; top panel) and total particle number concentrations (10–800 nm; PNC; bottom panel) (Lag 2–4). The x-axis shows the results for the main (displayed as dot), two-pollutant (displayed as rectangle), and effect modification analysis (displayed as diamond). The y-axis represents the percent change of risk per interquartile range (IQR: difference between the 75th and 25th percentile; corresponds to the spread of the middle 50% of the data) increase in air pollution concentration. Standardization by IQR facilitates comparison between different pollutants. All estimates represent the pooled analysis of the measurement stations using multi-level random-effects models, adjusted for main model covariates. It should be noted that for the two-pollutant models $PM_{2.5}$ and $NO_2$, the station Leipzig-TROPOS was not included in the model (no air pollution data). Additionally, the station Leipzig-Mitte was not included in the $NO_2$ model because Spearman correlation coefficients were above 0.7.

compared to our analysis, this study used 20 nm as lower cut-off value for defining UFP exposure, different exposure lags, and stations. We cannot exclude that the particle chemical composition changed maybe being partially responsible for the differences in effect estimates.

Other studies have investigated the effects of UFP in single cities. Branis and colleagues reported for Prague, Czech Republic, increasing risks of cardiovascular and respiratory hospital admissions for several particle sizes fractions (Braniš et al., 2010). The highest risks were observed for an eight-day average of particles in the accumulation mode. An increase of 1,000 particles/$cm^3$ was associated with a RR of 1.33 [95% CI: 1.13; 1.58] and 1.16 [95% CI: 1.05; 1.29], for respiratory and cardiovascular hospital admissions, respectively. In addition, effects were also present at more immediate lags (lag 0, 1), particularly for cardiovascular hospital admissions or Aitken mode particles (Braniš et al., 2010). However, a different exposure assessment, a shorter time series of less than one year, and a different region must be considered when comparing the results of Branis and colleagues with our results. A study conducted in London, UK, found higher but insignificant results for PNC, indicating stronger effects on pediatric respiratory hospital admissions (Samoli et al., 2016b). For respiratory hospital admissions, the authors reported a percent change in RR of 1.86% [95% CI: −0.28%; 4.05%] per IQR increase of PNC. Cardiovascular hospital admissions also showed positive but insignificant results (Samoli et al., 2016b). However, the time series included only the years 2011–2012, and different methods make it difficult to compare the results consistently to our study.

Our analysis observed different risk patterns for different particle size fractions. Generally, larger particle size fractions showed stronger delayed risks, highest for Aitken mode and accumulation mode particles (Fig. 2). These results are supported by the consistent results for $PM_{2.5}$. $PM_{2.5}$ represents the largest particles in our analysis, and although they are measured differently (mass concentration, not particle number concentration), we were able to validate our results showing the larger effects on hospital admissions for the larger particles. In contrast, for cardiovascular hospital admissions and hospital admissions for heart disease, we also found indications of immediate effects, but for smaller particle size fractions. Two studies using size-resolved particle metrics in Beijing, China, and Prague, Czech Republic, also found higher risks for larger particle size fractions with the strongest associations for accumulation mode particles (Braniš et al., 2010; Leitte et al., 2011). However, Branis and colleagues also reported associations between nucleation mode particles and respiratory hospital admissions (Braniš et al., 2010), which we did not observe in our study. Nevertheless, different size classifications (e.g., NuMP: 14.6–48.7 nm vs. 10–30 nm) make it difficult to compare the results consistently, because even small changes in cut-off values can have large effects on particle number (especially in the lower size range). A short-term study from Beijing, China, found significantly higher risks of cardiovascular emergency room visits in association with an 11-day moving average for the size fraction of 10–30 nm and 30–50 nm but no significant effects for shorter exposure lags or larger particle size fractions (Liu et al., 2013). Interestingly, we found significant heterogeneity in the smaller size fractions (e.g., cardiovascular hospital admissions and the size fraction of 10–30 nm; respiratory hospital admissions and the fraction 50–70 nm, Supplementary Table 7), triggered by the Augsburg results (data not shown). Using fixed-effects models (that consider less the heterogeneity

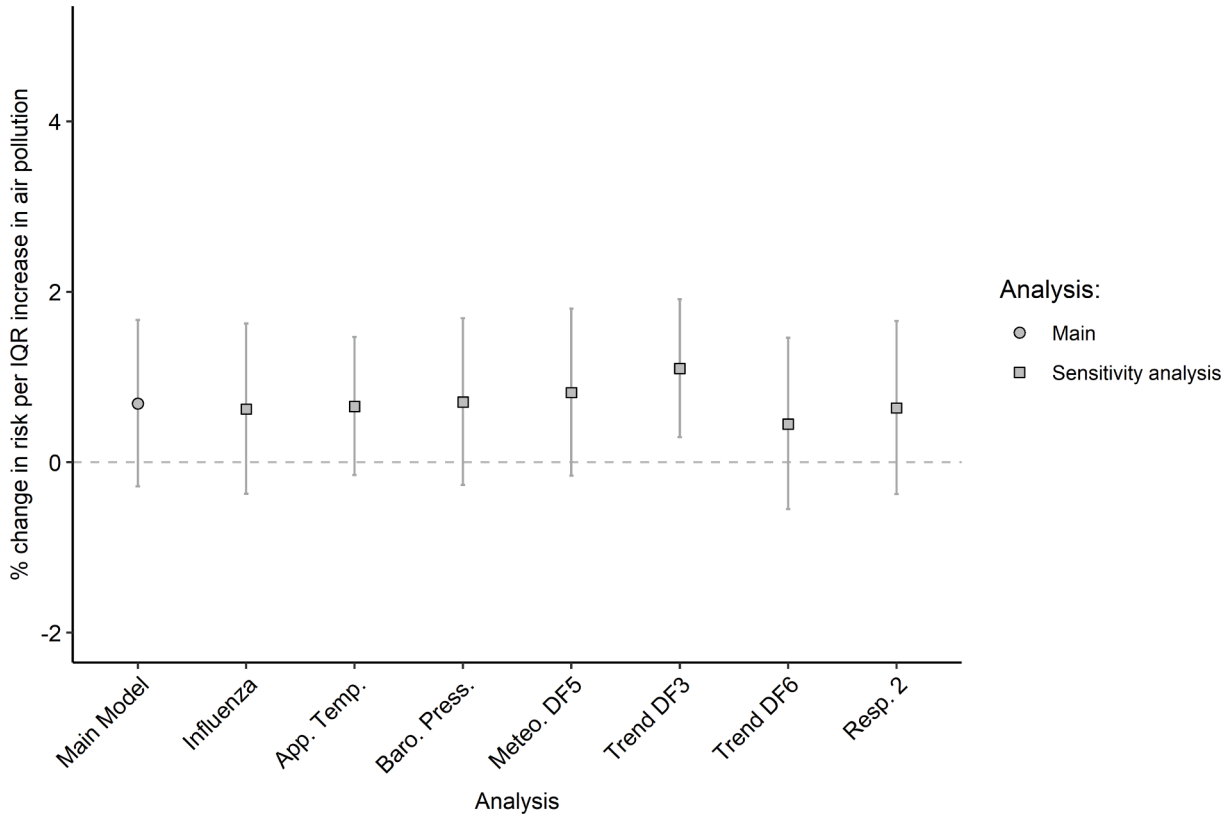


**Fig. 4.** Percent changes in the relative risk of respiratory hospital admissions and 95% confidence interval per interquartile range increases in ultrafine particles (10–100 nm; UFP) (Lag 2–4). The x-axis shows the results of the main model (displayed as dot) and different sensitivity analysis (displayed as rectangle). The y-axis represents the percent changes of risk per interquartile range (IQR: difference between the 75th and 25th percentile; corresponds to the spread of the middle 50% of the data) increase in air pollution concentration. Standardization by IQR facilitates comparison between different pollutants. All estimates represent the pooled analysis of the measurement stations using multi-level random-effects models, adjusted for main model covariates.

between the stations) also showed associations for particles in the Aitken mode size range (Supplementary Fig. 3 and Supplementary Table 9). Unfortunately, we could not validate this issue with data from another region and therefore highlight the suggestive character of our findings. We can only hypothesize that different prevailing exposure sources could cause these differences. This would fit with the wider range of UFP particles, and the higher median concentrations observed in Augsburg, possibly indicating different sources (Table 2). In the study by Samoli and colleagues, source apportionment (via Positive Matrix Factorization) was used to identify four best-fit profiles of PSD origin (Samoli et al., 2016b). However, no significant associations were found for age-segregated cardiovascular or respiratory hospital admissions (Samoli et al., 2016b). Nevertheless, a higher risk was reported for traffic-related sources and cardiovascular hospital admissions (Lag 1; age 15–64 years) and for nucleation or urban background sources (Lag 2; age 0–14 years) and respiratory hospital admissions. Traffic-related sources had a distribution mode of around 30 nm, whereas regional nucleation and urban background sources showed modes around 20 nm and 70 nm, respectively (Samoli et al., 2016b). However, our study could only hypothesize different sources according to particle size because no source apportionment was conducted.

Only a few studies reported potential effect modification, primarily investigating differences between age categories. Three short-term studies (Belleudi et al., 2010; Samoli et al., 2016a; Samoli et al., 2016b) and two systematic reviews (Ohlwein et al., 2019; Samoli et al., 2020) reported higher respiratory hospital admissions of different causes for younger people, especially children. Our results are consistent with those findings, indicating the highest risk in the age category 0–17 years. Children spend more time active and outdoors and are therefore more exposed to air pollution (Bateson and Schwartz, 2007). Moreover, early-life developmental differences such as an immature immune system or different breathing patterns may make children more vulnerable than older people (Bateson and Schwartz, 2007). In contrast, Lanzinger and colleagues reported a higher risk for older people (Lanzinger et al., 2016). Higher risks of cause-specific hospital admissions have been reported for the warmer season (Ohlwein et al., 2019; Samoli et al., 2016a; Samoli et al., 2020). Our results showed no significant effect modification by temperature, although the cold season indicated stronger effects. A similar finding was observed by Lanzinger and colleagues (Lanzinger et al., 2016). A possible explanation could be differences in the exposure mix, a more substantial influence of lower temperatures, or less dilution of the air in the atmosphere. In particular, meteorological variables seem to play a role in particle formation processes for traffic-generated particles, and concentrations might be higher in the cold season (Vu et al., 2015). Finally, we did not find differences between men and women. Only one multi-city study investigated modifying effects of sex, observing comparable results between men and women (Lanzinger et al., 2016), similar to our findings.

Until today, it remains controversial whether the adverse health effects of ultrafine particles occur independently of those of fine particles. Although UFP/PNC represents a subfraction of $PM_{2.5}$, sources and temporal-spatial patterns may differ. As a result, high UFP/PNC concentrations do not mean high $PM_{2.5}$ concentrations (and vice versa), leading to limited representativeness and almost no relationship between the two quantities (de Jesus et al., 2019). Our results suggest independent UFP effects of other particulate air pollutants (e.g., $PM_{2.5}$ and BC) because the effects did not change substantially, and the confidence interval for $PM_{2.5}$ narrowed slightly. However, the interpretation of results from two-pollutant models is not intuitive and straightforward, especially when air pollutants share similar primary

sources and therefore could reflect more general effects of, e.g., combustion-related exposure mixtures. However, we did not see high correlations between the pollutants that would affect the correct attribution of the observed effects. In addition, although some pollutants have similar sources, they could differ in terms of characteristics, such as chemical composition. Nevertheless, without further investigation and characterization of UFP, we cannot exclude the possibility that our findings for UFP are influenced by other factors of air pollution or residual confounding. Further adjustment for $NO_2$ resulted in null results and thus increased uncertainty. This observation would support the assumption that UFP may be more closely linked to traffic-related exposures such as $NO_x$ or CO (Cassee et al., 2019) and highlights the potential importance of considering traffic-related factors when examining the health effects of UFP in populations. Recently, a review concluded that $NO_2$ adjustment had the most pronounced effect on UFP effects when adjusting for other co-pollutants (Ohlwein et al., 2019). High correlations and similar distribution patterns of UFP with other pollutants from the same source may lead to more unstable models and more biased effect estimates (e.g., multicollinearity or methodological issues) (Ohlwein et al., 2019). In addition, effect transfer could be present in multi-pollutant models when measurement error is present, leading to a higher attenuation of effects estimates for the pollutant with the higher error (Evangelopoulos et al., 2021). Future research could address this issue by implementing chemical composition or source-specific analyses in large epidemiological contexts with multiple monitoring stations per city. In addition, spatiotemporal modeling of UFP could contribute to more comprehensive and personalized exposure assessment. However, the high spatial variability of UFP and the simultaneous presence of multiple pollutants remains a challenge and a target for future research. For example, a recent study in the New York State, USA, reported delayed adverse effects of modeled UFP concentrations on cardiovascular hospital admissions, although concerns on the model resolution accuracy remains (Lin et al., 2022).

In the analysis by Samoli and colleagues, different effects on pediatric respiratory hospital admissions were observed for urban background particles (0.51% [95% CI: −1.39%; 2.45%]) compared with traffic sources (-0.20% [95% CI: −2.38%; 2.03%]) (Samoli et al., 2016b). On an exploratory basis, our analysis compared risks for two different underlying exposure patterns (urban background vs. traffic-related). In general, we found mostly comparable results between station types, although the analyses with traffic-related stations yielded slightly higher risk estimates. However, concentrations at urban background stations are assumed to better represent a city's population. In addition, to account for peak concentrations in pollutant levels more accurately, we included LMI and DDN as two traffic-related stations. However, a different local exposure composition could influence the estimates between, but also within, a city. For example, nucleation events or the formation of new particles can occur in locations with high solar irradiation, contributing notably to the PSD. For future research, this differentiation between station types may provide additional insights in situations where source apportionment is not possible, but the results need to be interpreted cautiously. To date, measurement of PSD has usually been conducted at sites where measurement infrastructure is already in place (e.g., routine monitoring of $PM_{2.5}$ or $NO_2$). However, it is unclear whether these locations are also adequate to represent the risk of spatially variable exposures such as UFP to the population. If future research consolidates evidence of adverse UFP effects independent of fine PM, current regulatory air quality monitoring standards would no longer be adequate. These inherently assume a good representation of UFP health effects by monitoring mass concentrations of the larger PM fraction (e.g., $PM_{2.5}$ and $PM_{10}$).

Three main potential pathways are hypothesized that, in combination, could promote adverse health effects of particulate air pollution (Rückerl et al., 2011). First, changes in cardiac autonomic tone are generally the first and most immediate response to the inhalation of air pollution and involve multiple reflex arcs (Perez et al., 2015). These alterations are directly triggered by stimulated neuronal reflexes that lead to changes in cardiac autonomic regulation (Rückerl et al., 2011). Second, after inhalation, UFP can enter the interstitium by transcytosis across epithelial cells of the alveoli and eventually enter the circulation, where they translocate from the lung throughout the body to distant non-pulmonary regions (Oberdörster et al., 2005; Rückerl et al., 2011). UFP can absorb toxic chemical compounds more easily because of their large surface area per unit mass and surface reactivity (Kwon et al., 2020). These substances can be transported throughout the body, leading to further damage. Third, subclinical systemic responses such as the release of pro-oxidative and pro-inflammatory mediators can be induced, leading to several inflammatory processes throughout the body, promoting endothelial dysfunction, a pro-coagulation state, and triggering pro-thrombotic effects (Brook et al., 2010; Rückerl et al., 2011).

In general, the epidemiological evidence can only provide rather suggestive evidence for cause-specific hospital admissions (except for the more consistent findings for children and larger particles such as $PM_{2.5}$). However, clinical relevance is given, as adverse health effects may already occur at a subclinical state (e.g., heart rate variability or systemic inflammation) and studies have already shown associations with UFP (Ohlwein et al., 2019).

## 5. Strengths and limitations

This study represents one of the so far few carefully designed multi-city studies implementing a harmonized exposure design over eight consecutive years. The GUAN and its operators ensured a high degree of standardization to measure PSD data with routine calibration and maintenance procedures of all devices. To our knowledge, for the first time in a multi-city epidemiological context, we included and compared monitoring stations with different exposure settings to better capture peak concentrations and thus more adequately represent the exposure situation in the cities. We thoroughly adjusted for confounders to rule out influences from time trends or meteorological variables, e.g., using apparent temperature as an alternative measure of the thermal environment does not lead to different results. A large number of sensitivity analyses demonstrated the robustness and conservativeness of our main results with respect to changes in the model. Several limitations must be acknowledged. First, as we performed multiple analyses, we cannot rule out that some of our results may have been caused by chance. As seen for additional $NO_2$ adjustment or adjustment for time trend with fewer degrees of freedom, residual confounding could be present, especially when originating from similar sources, as real-world air pollution is a complex mixture of different particles and gases. In general, the possibility of residual confounding cannot be ruled out because of the complex nature of UFP and the observational study design itself. Second, we did not have source-specific information on different air pollutants and could only assume their origin using particle size fractions, different particle size modes, or station types. In addition, local exposure compositions or influences (e.g., nucleation events or prevailing exposures in warm or cold period) may play an important role that will only be accurately characterized with further source or composition analyses. Therefore, it remains an open question whether the observed health effects are due to the particle number concentration per se, and a more detailed characterization of the PSD is needed to further investigate this issue. Schmid and Stoeger highlighted that surface area might play an important biological role, as it represents the area where other molecules can interact with tissues or fluids (Schmid and Stoeger, 2016). However, to optimally display the related aerosol exposure risk, multiple dose metrics should be included in analyses (Schmid and Stoeger, 2016). Third, unlike $PM_{2.5}$, UFP exhibits a higher spatial and temporal variation, which can lead to measurement error or exposure misclassification and limit the statistical strength of the association, especially when monitoring campaigns are adapted from those of larger and, therefore, more spatially homogeneous particles (HEI Review Panel on

Ultrafine Particles, 2013). This would be even more prominent if only one station were used to assess the exposure risk for an entire city. However, a study by Cyrys and colleagues (Cyrys et al., 2008) showed for Augsburg, Germany, that one carefully selected urban background station can adequately characterize the temporal variation in a city. However, we included only six stations, which may result in a lack of statistical power, e.g., the number of cities may not be sufficient to detect health effects for the smallest particles, and we did not statistically correct for measurement error and its potential impact on the results (van Smeden et al., 2019). In addition, a more in-depth consideration of potential measurement error, especially in multi-pollutant models, can help to quantify the health effects and interdependency of different air pollutants more correctly since effect transfer could occur leading to an underestimation of the true independent health effect for the pollutant with the higher measurement error (Evangelopoulos et al., 2021). Fourth, the number of cases in the population for some cause-specific endpoints were rather low (e.g., cerebrovascular hospital admissions), although no large uncertainty was seen in the confidence intervals. In addition, due to data protection regulations, the exact location of each hospital admission was not available. We therefore had to assume that individuals living in a city were likely to be hospitalized in the same city/region, leading to only a small degree of uncertainty. Last, only German locations were included, which should be considered when comparing the results with other studies. For example, meteorological or climatic conditions could have an influence on ambient UFP concentrations (e.g., wind speed or precipitation), calling for further multi-country or multi-city studies.

## 6. Conclusion

In summary, this time series analysis found no clear pattern of associations for UFP or PNC with cause-specific hospital admissions. However, we found clear associations for $PM_{2.5}$ and suggestive delayed effects were seen for respiratory hospital admissions and multi-day averages of 2 to 4 days. In addition, the effects of different particle size fractions seemed to be larger for Aitken mode particles and strongest for accumulation mode particles, which is in line with the findings for $PM_{2.5}$. Furthermore, children showed the highest risk with respect to UFP exposure and higher effects were seen in the cold season. Different methodological approaches for exposure and statistical assessment (e.g., measurement routines, devices, lag structures, and classification of particles) and the overall still scarce evidence contribute to difficulties in assessing the overall evidence. Future research would greatly benefit from further standardization of methods; first, initial recommendations were published by the World Health Organization in 2021 (see “Good practice statement – UFP” (World Health Organization, 2021)).

**Funding:**

This work was supported by grants from the Saxon State Office for Environment, Agriculture and Geology (LfULG), Dresden, Germany.

## Declaration of Competing Interest

The authors declare that they have no known competing financial interests or personal relationships that could have appeared to influence the work reported in this paper.

## Data availability

The authors do not have permission to share data.

*Acknowledgements*

Source for hospital admission data: RDC of the Federal Statistical Office and Statistical Offices of the Federal States, Hospital Statistics [EVAS 23131], survey years [2010-2017], DOI: 10.21242/23131.2010.00.02.1.1.0 to 10.21242/23131.2017.00.02.1.1.0, own calculations.

The authors thank Karen Meyer (Research Data Centre of the Federal Statistical Office and Statistical Offices of the Federal States (FDZ), Fürth, Germany) for support with the hospital admission data. We thank Maik Merkel (Leibniz Institute for Tropospheric Research (TROPOS), Leipzig, Germany) for providing data of Leipzig-TROPOS, and Andrea Hausmann and Gunter Löschau for advice with the study concept. Finally, we thank the editors and unknown reviewers for their thoughtful comments and suggestions on the manuscript.

## Appendix A. Supplementary data

Supplementary data to this article can be found online at https://doi.org/10.1016/j.envint.2023.108032.

## References

Atkinson, R.W., Kang, S., Anderson, H.R., Mills, I.C., Walton, H.A., 2014. Epidemiological time series studies of PM2.5 and daily mortality and hospital admissions: a systematic review and meta-analysis. Thorax 69 (7), 660–665.

Bateson, T.F., Schwartz, J., 2007. Children’s response to air pollutants. J. Toxicol. Environ. Health A 71 (3), 238–243.

Belleudi, V., Faustini, A., Stafoggia, M., Cattani, G., Marconi, A., Perucci, C.A., Forastiere, F., 2010. Impact of fine and ultrafine particles on emergency hospital admissions for cardiac and respiratory diseases. Epidemiology 21 (3), 414–423.

Berglind, N., Bellander, T., Forastiere, F., von Klot, S., Aalto, P., Elosua, R., Kulmala, M., Lanki, T., Löwel, H., Peters, A., Picciotto, S., Salomaa, V., Stafoggia, M., Sunyer, J., Nyberg, F., group, f.t.H.s., 2009. Ambient air pollution and daily mortality among survivors of myocardial infarction. Epidemiology 20, 110–118.

Birmili, W., Sun, J., Weinhold, K., Merkel, M., Rasch, F., Wiedensohler, A., Bastian, S., Löschau, G., Schladitz, A., Quass, U., Kuhlbusch, T.A.J., Kaminski, H., Cyrys, J., Pitz, M., Gu, J., Kusch, T., Flentje, H., Meinhardt, F., Schwerin, A., Bath, O., Ries, L., Gerwig, H., Wirtz, K., Weber, S., 2015. Atmospheric aerosol measurements in the German Ultrafine Aerosol Network (GUAN) - Part III: black Carbon mass and particle number concentrations 2009–2014. Gefahrst. Reinh. Luft. 75, 479–488.

Birmili, W., Weinhold, K., Rasch, F., Sonntag, A., Sun, J., Merkel, M., Wiedensohler, A., Bastian, S., Schladitz, A., Löschau, G., Cyrys, J., Pitz, M., Gu, J., Kusch, T., Flentje, H., Quass, U., Kaminski, H., Kuhlbusch, T.A.J., Meinhardt, F., Schwerin, A., Bath, O., Ries, L., Gerwig, H., Wirtz, K., Fiebig, M., 2016. Long-term observations of tropospheric particle number size distributions and equivalent black carbon mass concentrations in the German Ultrafine Aerosol Network (GUAN). Earth Syst. Sci. Data 8, 355–382.

Braniš, M., Vyškovská, J., Malý, M., Hovorka, J., 2010. Association of size-resolved number concentrations of particulate matter with cardiovascular and respiratory hospital admissions and mortality in Prague, Czech Republic. Inhal. Toxicol. 22 (sup2), 21–28.

Brook, R.D., Rajagopalan, S., Pope, C.A., Brook, J.R., Bhatnagar, A., Diez-Roux, A.V., Holguin, F., Hong, Y., Luepker, R.V., Mittleman, M.A., Peters, A., Siscovick, D., Smith, S.C., Whitsel, L., Kaufman, J.D., 2010. Particulate matter air pollution and cardiovascular disease. Circulation 121 (21), 2331–2378.

Brunekreef, B., Strak, M., Chen, J., Andersen, Z., Atkinson, R., Bauwelinck, M., Bellander, T., Boutron, M., Brandt, J., Carey, I., Cesaroni, G., Forastiere, F., Fecht, D., Gulliver, J., Hertel, O., Hoffmann, B., de Hoogh, K., Houthuijs, D., Hvidtfeldt, U., Janssen, N., Jørgensen, J., Katsouyanni, K., Ketzel, M., Klompmaker, J., Krog, N., Liu, S., Ljungman, P., Mehta, A., Nagel, G., Oftedal, B., Pershagen, G., Peters, A., Raaschou-Nielsen, O., Renzi, M., Rodopoulou, S., Samoli, E., Schwarze, P., Sigsgaard, T., Stafoggia, M., Vienneau, D., Weinmayr, G., Wolf, K., Hoek, G., 2021. Mortality and morbidity effects of long-term exposure to low-level PM(2.5), BC, NO(2), and O(3): an analysis of european cohorts in the ELAPSE project. Res. Rep. Health Eff. Inst. 1–127.

Cassee, F., Morawska, L., Peters, A., Wierzbicka, A., Buonanno, G. , Cyrys, J., SchnelleKreis, J., Kowalski, M., Riediker, M., Birmili, W., Querol, X., Yildirim, A., Elder, A., Yu, I., Øvrevik, J., Hougaard, K., Loft, S., Schmid, O., Schwarze, P., Stöger, T., Schneider, A., Okokon, E., Samoli, E., Stafoggia, M., Pickford, R., Zhang, S., Breitner, S., Schikowski, T., Lanki, T., Aurelio, T. White Paper: Ambient ultrafine particles: evidence for policy makers.

Chen, J., Hoek, G., 2020. Long-term exposure to PM and all-cause and cause-specific mortality: a systematic review and meta-analysis. Environ. Int. 143, 105974.

Cyrys, J., Pitz, M., Heinrich, J., Wichmann, H.-E., Peters, A., 2008. Spatial and temporal variation of particle number concentration in Augsburg, Germany. Sci. Total Environ. 401 (1-3), 168–175.

da Costa e Oliveira, J.R., Base, L.H., de Abreu, L.C., Filho, C.F., Ferreira, C., Morawska, L., 2019. Ultrafine particles and children’s health: literature review. Paediatric Resp. Rev. 32, 73–81.

de Jesus, A.L., Rahman, M.M., Mazaheri, M., Thompson, H., Knibbs, L.D., Jeong, C., Evans, G., Nei, W., Ding, A., Qiao, L., Li, L., Portin, H., Niemi, J.V., Timonen, H., Luoma, K., Petaja, T., Kulmala, M., Kowalski, M., Peters, A., Cyrys, J., Ferrero, L., Manigrasso, M., Avino, P., Buonano, G., Reche, C., Querol, X., Beddows, D., Harrison, R.M., Sowlat, M.H., Sioutas, C., Morawska, L., 2019. Ultrafine particles and PM2.5 in the air of cities around the world: are they representative of each other? Environ. Int. 129, 118–135.

Evangelopoulos, D., Katsouyanni, K., Schwartz, J., Walton, H., 2021. Quantifying the short-term effects of air pollution on health in the presence of exposure measurement error: a simulation study of multi-pollutant model results. Environ. Health 20, 94.
HEI Review Panel on Ultrafine Particles. Understanding the Health Effects of Ambient Ultrafine Particles, 2013. HEI Perspectives 3. Boston, MA: Health Effects Institute.
Kwon, H.-S., Ryu, M.H., Carlsten, C., 2020. Ultrafine particles: unique physicochemical properties relevant to health and disease. Exp. Mol. Med. 52 (3), 318–328.
Lanzinger, S., Schneider, A., Breitner, S., Stafoggia, M., Erzen, I., Dostal, M., Pastorkova, A., Bastian, S., Cyrys, J., Zscheppang, A., Kolodnitska, T., Peters, A., group, U.s., 2016. Ultrafine and fine particles and hospital admissions in Central Europe. Results from the UFIREG study. Am. J. Respir. Crit. Care Med. 194, 1233–1241.
Leitte, A.M., Schlink, U., Herbarth, O., Wiedensohler, A., Pan, X.-C., Hu, M., Richter, M., Wehner, B., Tuch, T., Wu, Z., Yang, M., Liu, L., Breitner, S., Cyrys, J., Peters, A., Wichmann, H.-E., Franck, U., 2011. Size-segregated particle number concentrations and respiratory emergency room visits in Beijing, China. Environ. Health Perspect. 119 (4), 508–513.
Li, Q., Yi, Q., Tang, L., Luo, S., Tang, Y., Zhang, G., Luo, Z., 2019. Influence of ultrafine particles exposure on asthma exacerbation in children: a meta-analysis. Curr. Drug Targets 20 (4), 412–420.
Lin, S., Ryan, I., Paul, S., Deng, X., Zhang, W., Luo, G., Dong, G.-H., Nair, A., Yu, F., 2022. Particle surface area, ultrafine particle number concentration, and cardiovascular hospitalizations. Environmen. Pollut. 310, 119795.
Liu, L., Breitner, S., Schneider, A., Cyrys, J., Brüske, I., Franck, U., Schlink, U., Marian Leitte, A., Herbarth, O., Wiedensohler, A., Wehner, B., Pan, X., Wichmann, H.E., Peters, A., 2013. Size-fractioned particulate air pollution and cardiovascular emergency room visits in Beijing, China. Environ. Res. 121, 52–63.
Morawska, L., Ristovski, Z., Jayaratne, E.R., Keogh, D.U., Ling, X., 2008. Ambient nano and ultrafine particles from motor vehicle emissions: characteristics, ambient processing and implications on human exposure. Atmos. Environ. 42 (35), 8113–8138.
O'Neill, M.S., Zanobetti, A., Schwartz, J., 2003. Modifiers of the temperature and mortality association in Seven US cities. Am. J. Epidemiol. 157, 1074–1082.
Oberdörster, G., Oberdörster, E., Oberdörster, J., 2005. Nanotoxicology: an emerging discipline evolving from studies of ultrafine particles. Environ. Health Perspect. 113 (7), 823–839.
Ohlwein, S., Kappeler, R., Kutlar Joss, M., Künzli, N., Hoffmann, B., 2019. Health effects of ultrafine particles: a systematic literature review update of epidemiological evidence. Int. J. Public Health 64 (4), 547–559.
Orellano, P., Reynoso, J., Quaranta, N., Bardach, A., Ciapponi, A., 2020. Short-term exposure to particulate matter (PM10 and PM2.5), nitrogen dioxide (NO2), and ozone (O3) and all-cause and cause-specific mortality: systematic review and meta-analysis. Environ. Int. 142, 105876.
Perez, C.M., Hazari, M.S., Farraj, A.K., 2015. Role of autonomic reflex arcs in cardiovascular responses to air pollution exposure. Cardiovasc. Toxicol. 15 (1), 69–78.
Pfeifer, S., Birmili, W., Schladitz, A., Müller, T., Nowak, A., Wiedensohler, A., 2014. A fast and easy-to-implement inversion algorithm for mobility particle size spectrometers considering particle number size distribution information outside of the detection range. Atmos. Meas. Tech. 7, 95–105.
Rückerl, R., Schneider, A., Breitner, S., Cyrys, J., Peters, A., 2011. Health effects of particulate air pollution: a review of epidemiological evidence. Inhal. Toxicol. 23 (10), 555–592.
Samoli, E., Andersen, Z.J., Katsouyanni, K., Hennig, F., Kuhlbusch, T.A.J., Bellander, T., Cattani, G., Cyrys, J., Forastiere, F., Jacquemin, B., Kulmala, M., Lanki, T., Loft, S., Massling, A., Tobias, A., Stafoggia, M., 2016a. Exposure to ultrafine particles and respiratory hospitalisations in five European cities. Eur. Resp. J. 48 (3), 674–682.
Samoli, E., Atkinson, R.W., Analitis, A., Fuller, G.W., Beddows, D., Green, D.C., Mudway, I.S., Harrison, R.M., Anderson, H.R., Kelly, F.J., 2016b. Differential health effects of short-term exposure to source-specific particles in London, U.K. Environ. Int. 97, 246–253.
Samoli, E., Rodopoulou, S., Schneider, A., Morawska, L., Stafoggia, M., Renzi, M., Breitner, S., Lanki, T., Pickford, R., Schikowski, T., Enembe, O., Zhang, S., Zhao, Q.i., Peters, A., 2020. Meta-analysis on short-term exposure to ambient ultrafine particles and respiratory morbidity. Eur. Respir. Rev. 29 (158), 200116.
Schladitz, A., Merkel, M., Bastian, S., Birmili, W., Weinhold, K., Löschau, G., Wiedensohler, A., 2014. A concept of an automated function control for ambient aerosol measurements using mobility particle size spectrometers. Atmos. Meas. Tech. 7, 1065–1073.
Schmid, O., Stoeger, T., 2016. Surface area is the biologically most effective dose metric for acute nanoparticle toxicity in the lung. J. Aerosol Sci. 99, 133–143.
Schwarz, M., Schneider, A., Cyrys, J., Bastian, S., Breitner, S., Peters, A., 2023. Impact of ambient ultrafine particles on cause-specific mortality in three German cities. Am. J. Respir. Crit. Care Med. 207 (10), 1334–1344.
Sera, F., Gasparrini, A., 2022. Extended two-stage designs for environmental research. Environ. Health 21, 41.
Sera, F., Armstrong, B., Blangiardo, M., Gasparrini, A., 2019. An extended mixed-effects framework for meta-analysis. Stat. Med. 38 (29), 5429–5444.
Stafoggia, M., Samoli, E., Alessandrini, E., Cadum, E., Ostro, B., Berti, G., Faustini, A., Jacquemin, B., Linares, C., Pascal, M., Randi, G., Ranzi, A., Stivanello, E., Forastiere, F., 2013. Short-term associations between fine and coarse particulate matter and hospitalizations in southern Europe: results from the MED-PARTICLES project. Environ. Health Perspect. 121 (9), 1026–1033.
Stone, V., Miller, M.R., Clift, M.J.D., Elder, A., Mills, N.L., Møller, P., Schins, R.P.F., Vogel, U., Kreyling, W.G., Jensen, K.A., Kuhlbusch, T.A.J., Schwarze, P.E., Hoet, P., Pietroiusti, A., Vizcaya-Ruiz, A.D., Baeza-Squiban, A., Teixeira, J.P., Tran, C.L., Cassee, F.R., 2017. Nanomaterials Versus ambient ultrafine particles: an opportunity to exchange toxicology knowledge. Environ. Health Perspect. 125, 106002.
Sun, J., Birmili, W., Hermann, M., Tuch, T., Weinhold, K., Spindler, G., Schladitz, A., Bastian, S., Löschau, G., Cyrys, J., Gu, J., Flentje, H., Briel, B., Asbach, C., Kaminski, H., Ries, L., Sohmer, R., Gerwig, H., Wirtz, K., Meinhardt, F., Schwerin, A., Bath, O., Ma, N., Wiedensohler, A., 2019. Variability of black carbon mass concentrations, sub-micrometer particle number concentrations and size distributions: results of the German Ultrafine Aerosol Network ranging from city street to High Alpine locations. Atmos. Environ. 202, 256–268.
UFIREG Project, 2014. Handbook UFIREG Project.
van Smeden, M., Lash, T.L., Groenwold, R.H.H., 2019. Reflection on modern methods: five myths about measurement error in epidemiological research. Int. J. Epidemiol. 49, 338–347.
Vu, T.V., Delgado-Saborit, J.M., Harrison, R.M., 2015. Review: particle number size distributions from seven major sources and implications for source apportionment studies. Atmos. Environ. 122, 114–132.
Wiedensohler, A., Birmili, W., Nowak, A., Sonntag, A., Weinhold, K., Merkel, M., Wehner, B., Tuch, T., Pfeifer, S., Fiebig, M., Fjäraa, A.M., Asmi, E., Sellegri, K., Depuy, R., Venzac, H., Villani, P., Laj, P., Aalto, P., Ogren, J.A., Swietlicki, E., Williams, P., Roldin, P., Quincey, P., Hüglin, C., Fierz-Schmidhauser, R., Gysel, M., Weingartner, E., Riccobono, F., Santos, S., Grüning, C., Faloon, K., Beddows, D., Harrison, R., Monahan, C., Jennings, S.G., O'Dowd, C.D., Marinoni, A., Horn, H.G., Keck, L., Jiang, J., Scheckman, J., McMurry, P.H., Deng, Z., Zhao, C.S., Moerman, M., Henzing, B., de Leeuw, G., Löschau, G., Bastian, S., 2012. Mobility particle size spectrometers: harmonization of technical standards and data structure to facilitate high quality long-term observations of atmospheric particle number size distributions. Atmos. Meas. Tech. 5, 657–685.
Wiedensohler, A., Wiesner, A., Weinhold, K., Birmili, W., Hermann, M., Merkel, M., Müller, T., Pfeifer, S., Schmidt, A., Tuch, T., Velarde, F., Quincey, P., Seeger, S., Nowak, A., 2018. Mobility particle size spectrometers: calibration procedures and measurement uncertainties. Aerosol Sci. Technol. 52 (2), 146–164.
Wolf, K., Schneider, A., Breitner, S., von Klot, S., Meisinger, C., Cyrys, J., Hymer, H., Wichmann, H.-E., Peters, A., 2009. Air temperature and the occurrence of myocardial infarction in Augsburg, Germany. Circulation 120 (9), 735–742.
World Health Organization, 2021. WHO Global Air Quality Guidelines: Particulate Matter (PM2.5 and PM10), Ozone, Nitrogen Dioxide, Sulfur Dioxide and Carbon Monoxide. World Health Organization, Geneva.